The 4th International Conference on Structural Health Monitoring and Integrity Management

Design and Application of a Bandgap Meta-surface for Fatigue Damage Detection with Superharmonic Nonlinear Ultrasonic Technique

Yiran Tian[1] and Yanfeng Shen[1, *]

Abstract: This paper presents the design and application of a bandgap meta-surface to eliminate the influence from the inherent nonlinear sources in nonlinear ultrasonic inspection techniques, in order to achieve a baseline free, sensitive fatigue damage detection strategy. A meta-surface composed of aluminum-lead composite cylinders arranged in a periodic pattern on a host plate was designed. According to the local resonance (LR) mechanism, by adjusting the height ratio between the aluminum and lead cylinders, the bandgaps over desired frequency ranges can be opened up. Guided waves within the bandgap can be mechanically filtered out. A pitch-catch method was adopted to detect the fatigue cracks. The guided waves generated by a piezoelectric wafer active sensor (PWAS) propagate into the structure with inherent nonlinearity from the electronic devices and the adhesive layer under the transmitter. The guided waves will then propagate through the meta-surface, giving up the inherent second harmonic components. After the filtration, the interrogating waves will interact with the fatigue crack, acquire the second harmonic again, and are picked up by the receiver PWAS. The elimination of inherent second harmonic component from the interrogating wave field makes the diagnosis of the nonlinearity from the fatigue crack contact dynamics more accurately and clearly. During the meta-surface design stage, the dispersion curves and bandgap structure are investigated via the modal analysis of a unit cell with Bloch-Floquet boundary condition. Then, a finite element model (FEM) for a chain of unit cells is established to verify the bandgap effect. Finally, the pitch-catch active sensing procedure involving the meta-surface is modeled using the transient dynamic FEM simulation to obtain the response of the structure. The proposed technique is illuminated by comparing the second harmonic amplitude with the fatigue crack severity. The paper finishes with summary, concluding remarks, and suggestions for future work.

Keywords: Structural health monitoring, nondestructive evaluation, damage detection, metamaterial, nonlinear ultrasonics, fatigue cracks, higher harmonic, bandgap

[1]University of Michigan-Shanghai Jiao Tong University Joint Institute, Shanghai Jiao Tong University, 800 Dongchuan Road, Minhang District, Shanghai, 200240, China.

[*]Corresponding Author: Yanfeng Shen. Email: yanfeng.shen@sjtu.edu.cn.

1. Introduction

In recent years, local resonance based elastic metamaterials (EMMs) are drawing increasing attention among the structural health monitoring (SHM) and nondestructive evaluation (NDE) communities for their capability of wave/vibration manipulation. Many novel EMMS designs have been investigated since the first localized resonant (LR) sonic structure was realized by Liu et al. [Liu, Zhang, Mao et al. (2000)]. Wu et al. [Wu, Huang, Tsai et al. (2008)] demonstrated the existence of complete bandgaps in a plate with periodic stubbed surface. They analyzed the dispersion relation between Lamb waves and the stubbed surface to understand the effect of the heights of stubs on the band structure. Hsu et al. [Hsu and Wu (2007)] studied the propagation of Lamb waves in two-dimensional lattices composed of soft rubber embedded in an epoxy host. They achieved complete bandgaps in relatively low frequency ranges. And they proved the resonant frequencies of flexural modes depend on both the radius of the rubber cylinders and the thickness of the composite plate. Oudich et al. [Oudich, Li, Assouar et al. (2010)] investigated the acoustic properties of a two-layer composite structure bounded on a thin homogeneous plate. They obtained extremely low frequency bandgaps based on LR mechanism and illustrated that the width of such bandgap strongly depends on the height and cross section area of the stubs.

On the other hand, guided waves have been widely studied as a powerful tool for damage detection. The nonlinear ultrasonic technique has been proved to be sensitive to incipient changes in structures because of the distinctive features such as higher harmonics and subharmonics [Jhang (2009); Kruse (2009)]. Shen et al. [Shen and Giurgiutiu (2014)] conducted the research on the predictive modeling of nonlinear wave propagation for structural health monitoring with piezoelectric wafer active sensors. They introduced a Damage Index (DI) based on the amplitude ratio of the signal spectral harmonics to correlate the signal nonlinearity with damage severity. However, the identifiability of contact acoustic nonlinearity (CAN) from the wave crack interaction is always adversely influenced by the inherent nonlinear sources in engineering practice. These sources can be categorized into two classes: (a) inherent nonlinearity of the electronic equipment and (b) material nonlinearity (the hysteretic behavior of the adhesive between sensors and the aluminum plate). Thus, the nonlinear characteristics will always present in the sensing signal even for the pristine structures. To improve the accuracy of the diagnosis, the influence from the inherent nonlinear sources should be minimized.

This research investigates the design and application of a bandgap meta-surface to eliminate the inherent second harmonic for the purpose of improving the accuracy and reliability of nonlinear ultrasonic SHM and NDE for fatigue crack detection. After the introduction, the inherent nonlinearity will be demonstrated using pitch-catch active sensing signals. Then, the unit cell structure of the meta-surface will be designed, followed by the harmonic analysis for the demonstration of the bandgap phenomenon. Finally, the transient dynamic FEM simulation results for various damage severities will be presented to illustrate the capability of the meta-surface nonlinear SHM system for fatigue crack detection and quantification.

2. Inherent Nonlinearity in Pitch-catch Signals

The existence of the inherent nonlinear sources can be demonstrated via pitch-catch active sensing experiments. A pristine aluminum plate with a transmitter PWAS (T-PWAS) and a receiver PWAS (R-PWAS) was tested. Guided waves were excited at 50 kHz by the T-PWAS and sensing signal was captured by the R-PWAS. Figure 1a shows the continuous sinusoidal excitation signal centered at 50 kHz generated from the function generator before amplified by the amplifier. Figure 1b indicates that the frequency spectrum of the excitation only contains the fundamental frequency component. This excitation signal was further amplified by the amplifier, transduced into mechanical oscillations through the inverse piezoelectric effect, passed through the adhesive layer and the pristine aluminum plate, and was finally picked up by the R-PWAS. Figure 1c presents the time trace of the sensing signal. Figure 1d demonstrates that the higher harmonics are present in the sensing signal due to the inherent nonlinearity. Such inherent nonlinearity will influence the accuracy and identifiability of nonlinear ultrasonic inspections, because it is hard to distinguish the CAN from wave crack interaction from this noisy background. This paper strives to design and apply an ultrasonic bandgap meta-surface to remove such inherent influence from the interrogating waves for more accurate and reliable crack detection via nonlinear ultrasonic techniques.

In this study, only the second harmonic (100 kHz) and the third harmonic (150 kHz) are considered. The amplitude ratios of higher harmonics (100 kHz and 150 kHz) to the fundamental frequency (50 kHz) are recorded and used for our modeling task, in order to approximate the practical scenario.

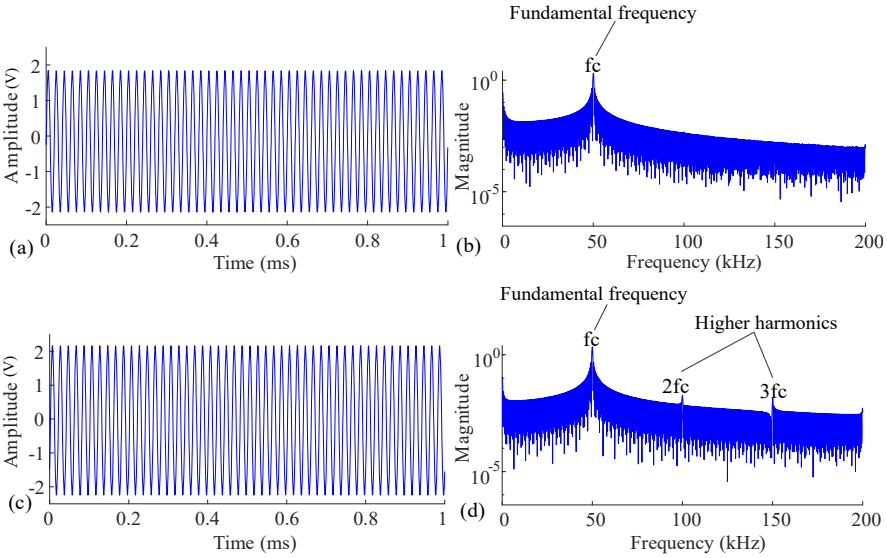

Figure 1: Signals from a pristine plate experiment: (a) time trace of the excitation signal; (b) frequency spectrum of the excitation signal; (c) time trace of the sensing signal; (d) frequency spectrum of the sensing signal

3. Design of Meta-surface Unit Cells

3.1. Computation of Dispersion Relations with Standard Finite Element Codes

Aberg et al. [Aberg and Gudmundson (1997)] put forward the methodology of utilizing standard finite element codes for computation of dispersion relations in materials with periodic microstructure. The periodicity means that the material is comprised of many finite-sized unit cells arranged in a regular pattern. By applying Bloch-Floquet constraints on the boundaries and corners of the unit cell, the dispersion relation representing the frequency-wavenumber domain can be calculated. Based on LR mechanism, when the excitation frequency approaches to the natural frequency of the resonators, the guided wave under this frequency cannot propagate through the structure, i.e., the corresponding frequency will not appear in the dispersion curve and bandgaps will develop. Figure 2a demonstrates the material and structural layout of the designed unit cell. Figure 2b presents the finite element model for the unite cell.

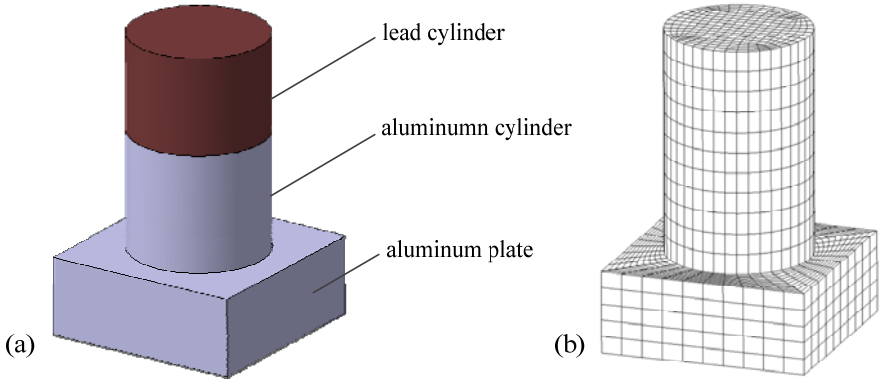

Figure 2: (a) Unit cell of the meta-surface; (b) unit cell finite element model

3.2. Dispersion Curve of the Meta-surface Structure

In this paper, the unit cell is composed of an aluminum-lead composite cylinder bounded on a host plate. According to the LR mechanism, by adjusting the height ratio between the aluminum and lead cylinders, the bandgaps over desired frequency ranges can be opened up. The height of aluminum cylinder is L and the height of the lead cylinder is l. The radius r of the stub is 1.75 *mm* and the lattice constant a of the unit cell is 5 *mm*. The total height of the stub is set to be 5.5 *mm*. The dispersion curves of the unit cells with different height ratios ($\eta = l / L$) are presented in Figure 3. From Figure 3a, it can be seen that there is no bandgap in the dispersion curve of a homogeneous host plate. By comparing the results shown in Figure 3(b)-(d), as the height ratio increases, the bandgap shifts to a higher range gradually. The bandgaps for different height ratios are shown in Figure 4. Considering this research, the second harmonic component (100 kHz) needs to be filtered away; the designed unit cell in Figure 3d shows desirable bandgap coverage over the target frequency range. In this case, the height of aluminum cylinder L is 3 *mm* and the height of lead cylinder l is 2.5 *mm*, i.e., the height ratio is 0.833, a desired wide

bandgap ranging from 95.53-109.6 kHz was achieved and it can be used to filter away the second superharmonic component in Figure 1d. Figure 5 shows the band structure of the meta-surface. The dispersion curves in all directions were calculated to examine and ensure a complete bandgap. A complete bandgap ranging from 95.53-109.6 kHz still exists to satisfy the requirement.

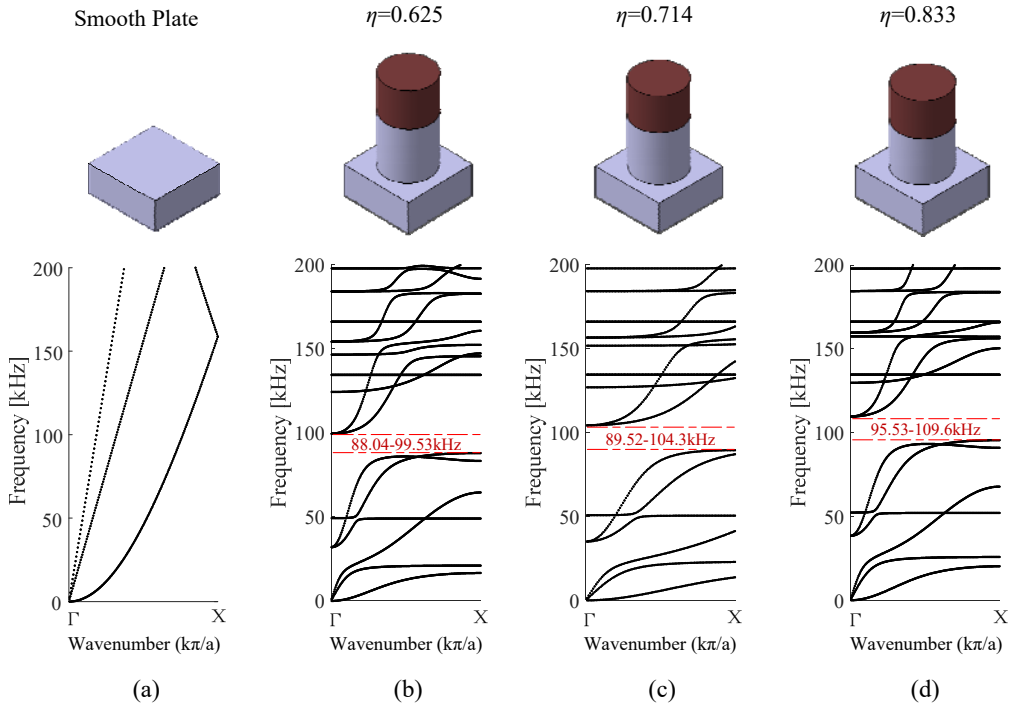

Figure 3: Unit cells with different aluminum and lead cylinder height ratios and the corresponding dispersion curves: (a) a smooth plate without stub; (b) meta-surface with a 0.625 height ratio; (c) meta-surface with a 0.714 height ratio; (d) meta-surface with a 0.833 height ratio

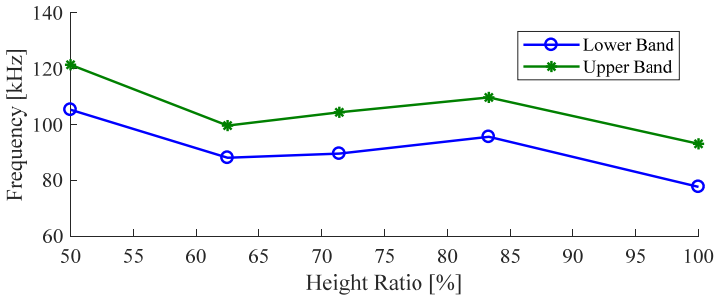

Figure 4: Bandgap features for the various height ratios

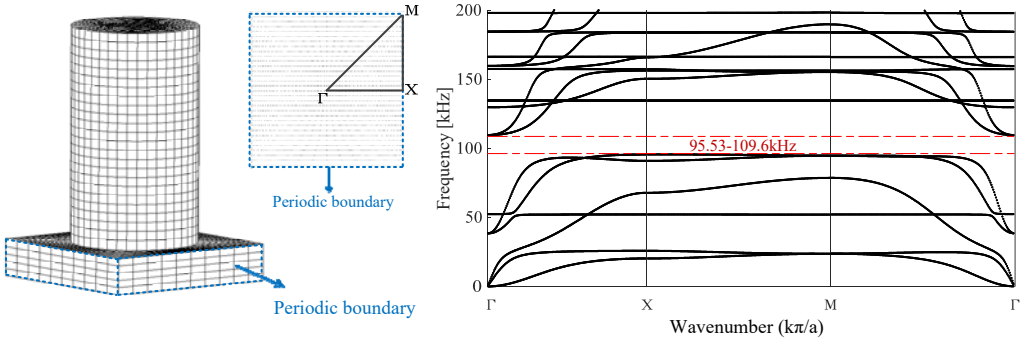

Figure 5: Band structure of the meta-surface

4. Spectral Response of the Meta-surface

4.1. Harmonic Analysis of a Chain of Unit Cells

Harmonic analysis was conducted to obtain the spectral response of the meta-surface structure and verify the bandgap effect from the unit cell design. A chain model which contains an array of 10×1 unit cells (Figure 3d) was constructed in ANSYS package. A 50-N external force sweeping from 0 to 200 kHz was excited on the left boundary of the chain model. The displacement and equivalent stress responses of the structure corresponding to various excitation frequencies were observed. The detailed model setups are shown in Figure 6a. In theory, as the frequency range of the external force falls within the bandgap, the first few unit cells may have the responses, however, the other ones should not, i.e., the guided waves cannot pass through the meta-surface structure.

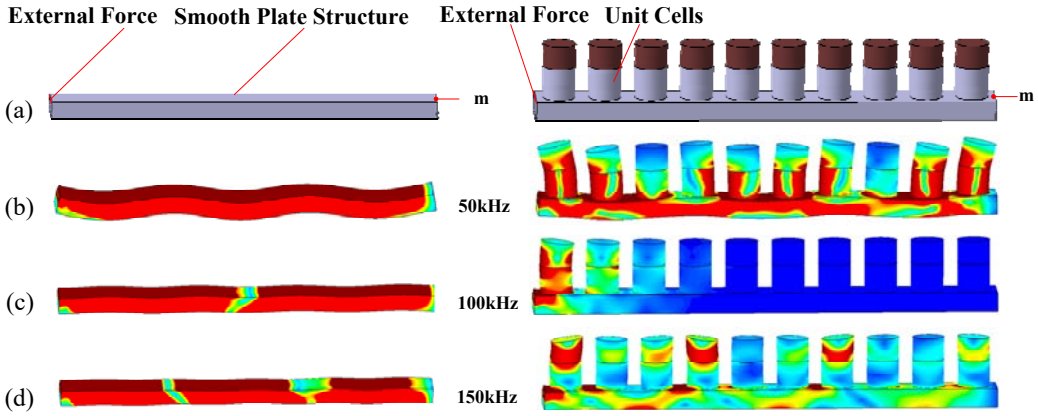

Figure 6: The designed structure with an array of 10×1 unit cells and the equivalent stress under different frequencies: (a) a simple plate strip and the meta-surface structure; (b) wavefield at 50 kHz; (c) wavefield at 100 kHz; (d) wavefield at 150 kHz

4.2. Simulation Results

Figure 6(b)-(c) show the equivalent stress responses of the meta-surface structure and the smooth plate at different frequencies, which are 50 kHz, 100 kHz and 150 kHz. The results demonstrate that when the external forces are excited at the fundamental frequency and the third superharmonic frequency which are both out of the bandgap, the equivalent stress of the two structures are all very large, i.e., the guided wave can pass through the whole structure in these cases. By comparison, when the frequency of the external force is 100 kHz corresponding to the second higher harmonic within bandgap, the equivalent stress only appears in the first three unit cells, which means the meta-surface structure has the capability to prevent the guided waves propagating through the meta-surface structure.

Figure 7 shows the comparison between the in-plane displacement spectral responses and dispersion curves of the two structures. The results conclude that for meta-surface structure when the excitation frequency range is within the bandgap, the amplitude of the in-plane displacement reaches the minimum amplitude in the order of 1E-8. In comparison, this phenomenon does not appear in the homogeneous plate case. The structural spectral response agrees well with the bandgap predicted by the dispersion curves.

It should be noted that the target improved nonlinear ultrasonic inspection not only requires the elimination of the inherent second harmonic but also maintain the large interrogating wave amplitude at the fundamental frequency. Thus, particular attention was paid in the meta-surface design. It can be noticed in Figure 7b that the fundamental frequency components around 50 kHz renders very large response amplitudes. Thus, the current design enables the filtration of the inherent second harmonics while ensures the propagation of the interrogating wavefield at the fundamental frequency.

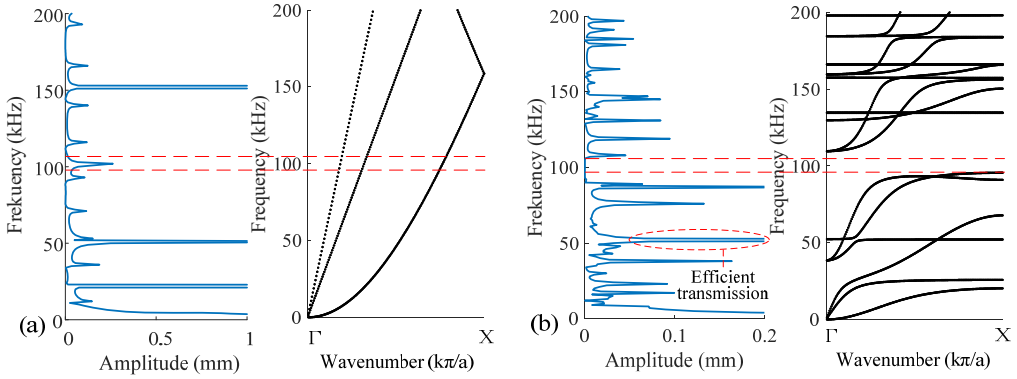

Figure 7: The results comparison between spectral response and band structure dispersion curve: (a) the smooth plate case; (b) meta-surface case

5. Numerical Simulation of Nonlinear Ultrasonic Active Sensing

5.1. Transient Dynamic Finite Element Model

Figure 8 exhibits the model layout of a pitch-catch active sensing procedure deploying the meta-surface. One 5-mm×5-mm×0.2-mm square T-PWAS was bounded on the left side of a 2-mm thick aluminum plate to generate guided waves. An array of 10×1 meta-surfaces was bounded on the aluminum plate 5 *mm* away from the T-PWAS. The crack was located at 65 *mm* from the transmitter behind the meta-surface. Another circular 3.5-mm diameter and 0.2-mm thickness PWAS was bounded on the right side of the crack at a 12.5-mm distance to receive the signals. To prevent the influence of the boundary reflections, non-reflective boundaries (NRB) were implemented on both ends of the plate trip. The T-PWAS would generate ultrasonic guided waves into the structure, carrying both the fundamental frequency waves (50 kHz) and superharmonic components (100 kHz, 150 kHz) from the inherent nonlinear sources. After the waves propagating through the meta-surfaces, the second harmonic participation at 100 kHz would be diminished. In a further step, the guided waves would interact with the crack, carrying crack information with them, and were finally picked up by the R-PWAS.

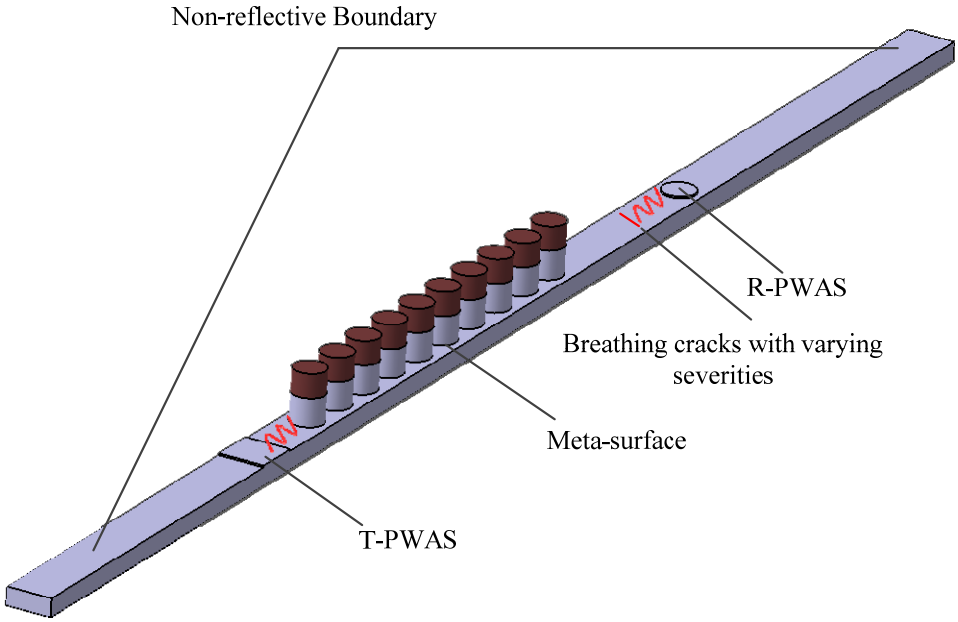

Figure 8: Model layout of pitch-catch active sensing with the meta-surface

To ensure the numerical accuracy and guarantee the efficiency of the simulation process, the element size and time step should be optimized. Hagedorn et al. [Hagedorn and Stadler (1988)] put forward the maximum element size l_e and time step Δt following

$$l_e = \frac{\lambda_{\min}}{20} \tag{1}$$

$$\Delta t = \frac{1}{20 f_{\max}} \tag{2}$$

where $\lambda_{\min}$ is the minimum wavelength and $f_{\max}$ is the maximum frequency.

The minimum wave length can be evaluated via the dispersion curves of the plate following Eq. (3)

$$\lambda = \frac{c}{f} \tag{3}$$

where λ is the wavelength, f represents the frequency, and c designates the wave speed. The wave speed can be calculated by solving the Rayleigh-Lamb equation and shown in Figure 9a. The wavelength is plotted in Figure 9b. From the result, A0 mode at 150 kHz possesses the minimum wavelength 10.31 *mm*. According to the equation (2) and (3), the maximum element size vs frequency and time step vs frequency relationships are relatively shown in Figure 9c and Figure 9d. At the third higher harmonic (150 kHz), the maximum mesh size is 0.5154 *mm*. So in our model, the maximum element size was set to be 0.5 *mm* to guarantee the spatial discretization requirement. From Figure 9d, the maximum allowable time-step is 0.33 μs. To satisfy such a condition, the time-step in our model was set to 0.3 μs. The length of the non-reflective boundary should be twice as long as the maximum wavelength. Hence, the length of the non-reflective boundary was set to be 40 *mm*.

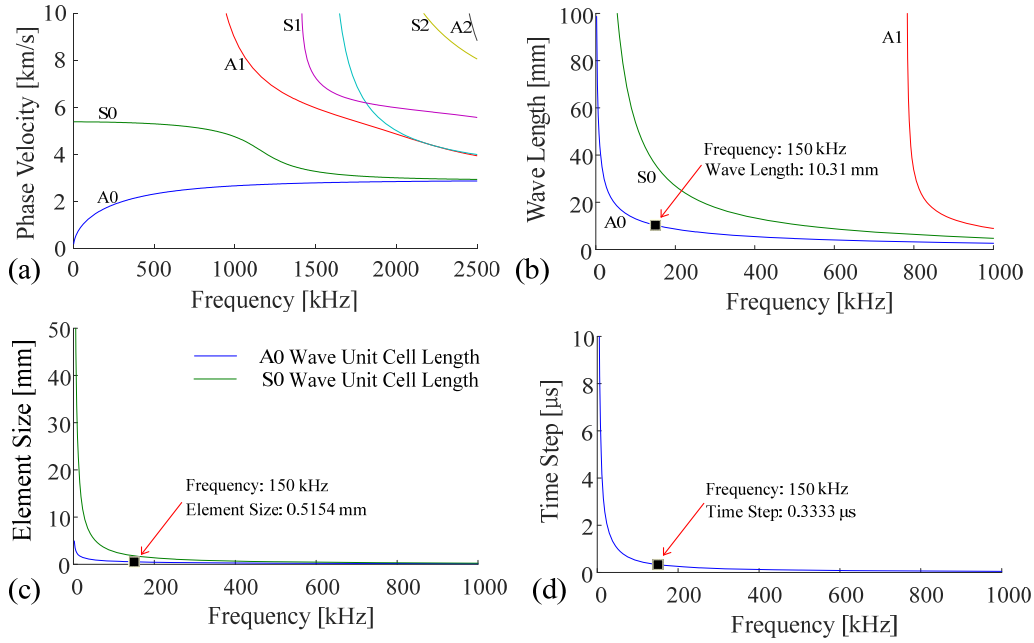

Figure 9: Discretization guidelines: (a) phase velocity dispersion curves; (b) wavelength dispersion curves; (c) frequency element size curve; (d) frequency time step curve

5.2. Case Study

In this section, the modeling results using the transient dynamic analysis for nonlinear ultrasonic pitch-catch active sensing procedure are presented.

5.2.1. The Pristine Case

A pristine plate was first investigated to demonstrate the effectiveness of the meta-surface design for inherent second harmonic filtration. Figure 10 shows the time trace of the excitation and sensing signals. The excitation signal contains three components which are 50 kHz, 100 kHz and 150 kHz. Figure 10d presents the frequency spectrum of the sensing signal at the R-PWAS. Figure 11 illustrates the time frequency features of the excitation and sensing signals. It can be noticed that the inherent higher harmonic components were present in the excitation signals, while the second harmonic component was successfully removed in the sensing signal. These results demonstrate that the proposed meta-surface can effectively eliminate the adverse influence from the inherent second harmonic. In this way, the appearance and magnitude of the second harmonic become evidently indicative of the nucleation and growth of fatigue cracks along the wave propagation path between the meta-surface and the R-PWAS.

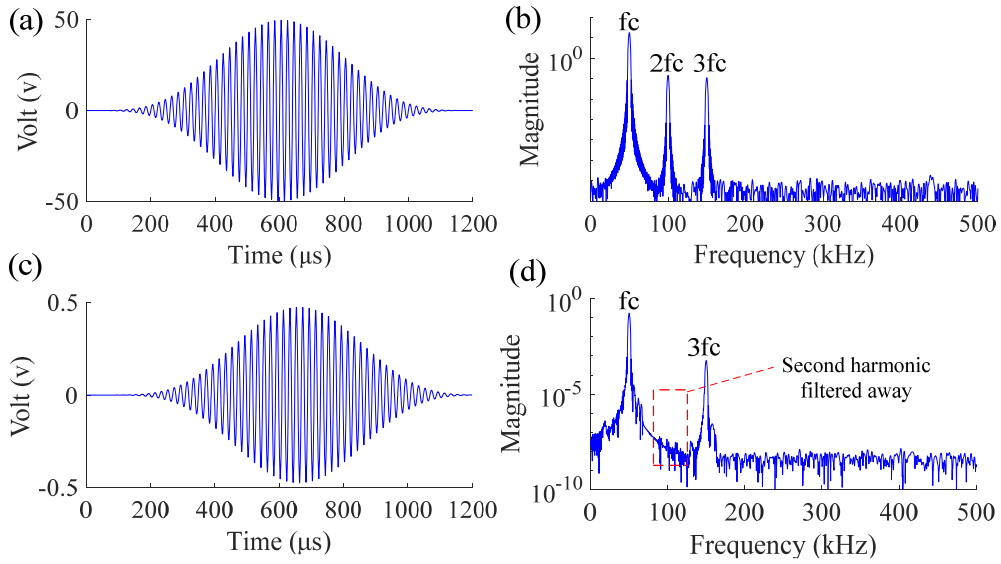

Figure 10: Pitch-catch active sensing signals: (a) time trace of the excitation; (b) frequency spectrum of the excitation contaminated by the inherent nonlinear superharmonics; (c) time trace of the sensing signal; (d) frequency spectrum of the sensing signal with the second harmonic eliminated by the meta-surface.

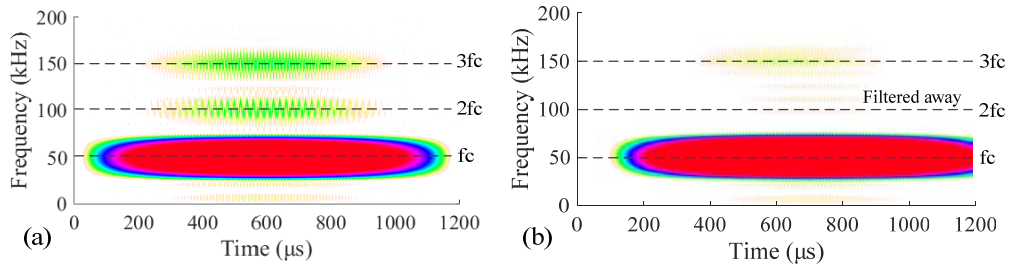

Figure 11: Time frequency representation of the signals: (a) excitation signal contaminated by the inherent nonlinear superharmonics; (b) sensing signal with the second harmonic eliminated by the meta-surface.

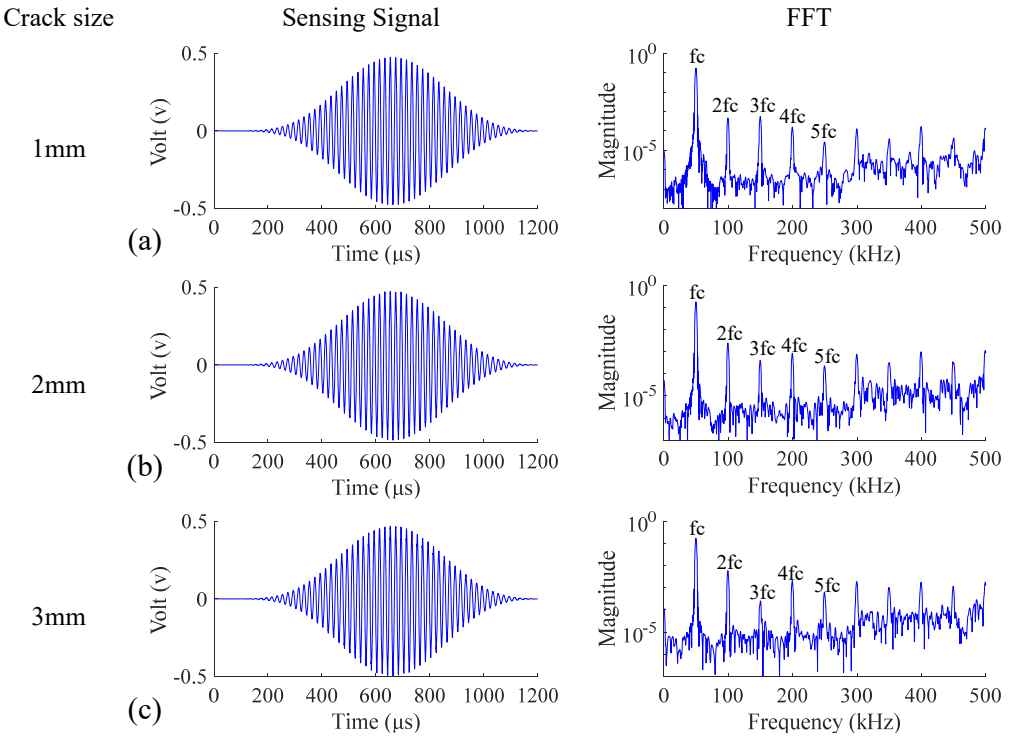

Figure 12: The time trace and frequency spectrum of the sensing signals: (a) 1-mm crack case; (b) 2-mm crack case; (c) 3-mm crack case

5.2.2. The Damaged Cases

The crack of various severities was introduced into the plate. The size of the crack increases gradually from 1 *mm* to 3 *mm* with a step of 1 *mm*. Figure 12(a)-(c) shows the frequency spectrum of the sensing signals in these three cases. It can be seen that in all three cases, the second higher harmonics appeared again after the guided waves interacting with the contact damage. Figure 13 shows the magnitude of the second higher

harmonic vs crack size. When the crack size increased, the amplitude of the second higher harmonic became larger. After applying time frequency analysis on the sensing signals of all three damage cases, the second higher harmonics appear again. Figure 14 presents the STFT result of the third damage case (3mm) as an example.

In conclusion, by comparing the results from 4.2.1 and 4.2.2 sections, the meta-surface enabled the filtration of the inherent nonlinearity and allowed the accurate, reliable identification and quantification of the fatigue crack.

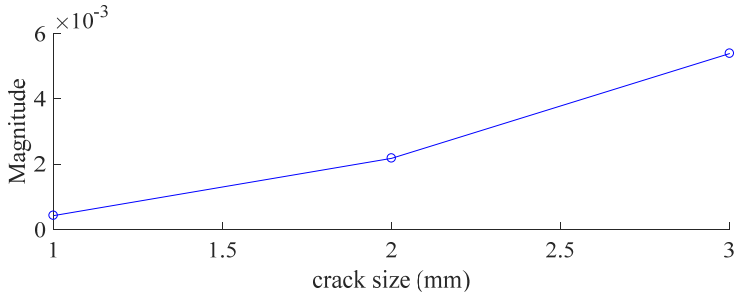

Figure 13: The magnitude of the second higher harmonic vs the crack size.

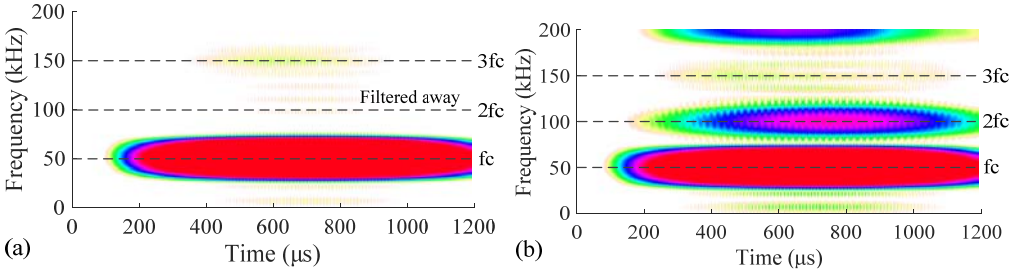

Figure 14: Time frequency representation of the sensing signals: (a) sensing signal for the pristine case; (b) sensing signal for the 3-mm crack case

6. Summary, Concluding Remarks, and Suggestions for Future Work

This paper presented a new method of using meta-surface for the improvement of nonlinear ultrasonic SHM and NDE. A meta-surface composed of aluminum-lead composite cylinders arranged in a periodic pattern on a host plate was designed. After optimization, this kind of meta-surface design can filter out the second harmonic component (100 kHz) introduced by the nonlinearity of the electronic instrument and the adhesives completely. By artificially adjusting the height ratio of different materials, the desired bandgap can be opened up. Harmonic analysis was performed to obtain the spectral response of the meta-surface. The bandgap feature was further verified. Within the bandgap, the oscillations caused by the external force can be removed when passing through the meta-surface.

Pitch-catch nonlinear ultrasonic NDE procedures were modeled for various damage severity cases. Inherent nonlinearities were considered in the excitation signal, containing

the first two nonlinear harmonics. The bandgap was set to cover the second higher harmonic around 100 kHz. The meta-surface was also designed to ensure the high pass of the interrogating waves at the fundamental frequency. In the pristine case, it was found that the designed meta-surface successfully filtered out the second higher harmonic, leaving merely the fundamental frequency and the third higher harmonic. Such a phenomenon helps to improve the identifiability of CAN from wave crack interactions. In the damaged cases, the results showed that after guided waves interacting with different sizes of cracks, the second higher harmonics appear again. It was also found that the amplitude of the second higher harmonic becomes larger with the increment of the crack size. The proposed method possesses great potential in future SHM and NDE applications.

For future work, nonlinear ultrasonic experiments with the designed meta-surface should be carried out. Various other designs of meta-surfaces should be explored for the purpose of improved SHM and NDE procedures.

Acknowledgement: The support from the National Natural Science Foundation of China (contract number 51605284) is thankfully acknowledged.

References:

Liu, Z. Y.; Zhang, X. X.; Mao, Y. W. (2000): Locally Resonant Sonic Materials. *Science,* vol. 289, no. 5485, pp. 1734–1736.

Wu, T. T.; Huang, Z. G.; Tsai, T. C. (2008): Evidence of complete band gap and resonances in a plate with periodic stubbed surface. *Applied Physics Letters,* vol. 93, no. 111902.

Hsu, J. C.; Wu, T. T. (2007): Lamb waves in binary locally resonant phononic plates with two-dimensional lattices. *Applied Physics Letters,* vol. 90, no. 201904.

Oudich, M.; Li, Y.; Assouar, M. B. (2010): A sonic band gap based on the locally resonant phononic plates with stubs. *New Journal of Physics,* vol. 12, no. 083049.

Jhang, K. Y. (2009): Nonlinear ultrasonic techniques for nondestructive assessment of micro damage in material: a review. *International Journal of Materials,* vol. 10, no. 1, pp. 123–135.

Kruse, W.; Zagrai, A. (2009): Investigation of linear and nonlinear electromechanical impedance techniques for detection of fatigue damage in aerospace materials. *7th international workshop on structural health monitoring,* Stanford, CA, 9-11 September.

Shen, Y. F.; Giurgiutiu, V. (2014): Predictive modeling of nonlinear wave propagation for structural health monitoring with piezoelectric wafer active sensors. *Journal of Intelligent Material Systems and Structures,* vol. 25, pp. 506–520

Aberg, M.; **Gudmundson, P**. (1997): The usage of standard finite element codes for computation of dispersion relations in materials with periodic microstructure, *Acoustical Society of America*. vol. 102.

Hagedorm, P.; **Stadler, W**. (1988): *Non-linear oscillations*, Oxford University Press, USA. vol. 10.